EurJIC
European Journal of Inorganic Chemistry

Research Article
doi.org/10.1002/ejic.202300023

Chemistry Europe
European Chemical Societies Publishing

www.eurjic.org

# Oxidorhenium(V) and Rhenium(III) Complexes with Arylselenolato and -tellurolato Ligands

Bruno Noschang Cabral,[a] Jéssica Fonseca Rodrigues,[a] Maximilian Roca Jungfer,[b] Anke Krebs,[b] Adelheid Hagenbach,[b] Ernesto Schulz Lang,*[a] and Ulrich Abram*[b]

*In situ* prepared lithium arylselenolates {LiSePh, LiSe(2,6-$Me_2$Ph), LiSe(2,4,6-$Me_3$Ph)} or -tellurolates {LiTePh, LiTe(2,6-$Me_2$Ph), LiTe(2,4,6-$Me_3$Ph)} react with $[ReOCl_3(PPh_3)_2]$ and $(NBu_4)Br$ in good yields under formation of rhenium(V) complexes of the composition $(NBu_4)[ReO(L)_4)]$. The first oxidorhenium(V) complex with four monodentate phenolato ligands, $[ReO(2,6\text{-}Me_2Ph)_4]^-$, was prepared and isolated in crystalline form. This allows a comparison of experimental and computational data of a full series of such compounds with basal O, S, Se and Te donor atoms. Similar reactions with $[ReCl_3(PPh_3)_2(CH_3CN)]$ or $[ReCl_3(PMe_2Ph)_3]$ give trigonal bipyramidal rhenium(III) complexes of the compositions $[Re(PPh_3)(L)_3(CH_3CN)]$ or $[Re(PPh_3)_2(L)_3]$ depending on the chalcogenolate applied. The reported oxidorhenium(V) and rhenium(III) complexes were fully characterized by spectroscopic methods and X-ray diffraction. The bonding situation in the rhenium(V) and rhenium(III) chalcogenolates was assessed through density functional theory calculations based on the quantum theory of atoms in molecules (QTAIM), natural bonding orbital (NBO) analysis, charge analysis, the electron localization function (ELF) maps and topological descriptors at the {3,−1} critical points such as metallicities. Expectedly, the ionicity of the rhenium-chalcogen bonds decreases according to all three applied charge models from O to Te. Generally, the Re–Se and Re–Te bonds are more directional in the Re(III) complexes than in the oxidorhenium(V) compounds.

## Introduction

Rhenium complexes possess a rich coordination chemistry in a wide range of oxidation states varying from −1 to +7.[1] Recent attention has been paid to complexes containing medium (+3) and high oxidation states (+5 and +7) as they can exemplarily be applied as catalysts in reactions such as oxygen-atom transfer or hydrosilylation agents.[2,3] Some of them are capable of reductive $N_2$ splitting to nitrido complexes and subsequent formation of ammonia.[4] Among the ligands used for such applications, aromatic organochalcogenolates ($ArE^-$ with E=O, S, Se or Te) represent an interesting and versatile class.[6–9] The coordination chemistry of rhenium complexes containing organothiolato ligands is well known with thoroughly performed structural studies and well explored synthetic pathways.[10–16] In contrast, there is a substantial lack of studies with monodentate phenolates or with ligands coordinating through heavier chalcogen donor atoms. Corresponding tellurium derivatives are especially scarce. This may mainly be due to the inherent instability of the precursor molecules. Only a few compounds containing Re–Se and Re–Te bonds have been crystallographically characterized and the majority of them contain rhenium in low oxidation states,[12,17–33] where phenylselenolates or -tellurolates act as bridging ligands between two tricarbonylrhenium(I) fragments.[21–33] Reports about well-defined rhenium(III) or rhenium(V) complexes containing arylselenolato or -tellurolato ligands are even more rare. In addition to some oxidorhenium compounds,[34–37] recently a series of phenylimido chelates of rhenium(V) has been reported with the corresponding diselenides and ditellurides as starting materials. Selective reduction of the dichalcogenides was performed by phosphines, which were released during the reaction of $[Re(NPhR)Cl_3(PPh_3)_2]$ complexes (R=H, F, $CF_3$) with the corresponding dichalcogenides.[38] A similar approach was also successful for a number of chelating selenolates and tellurolates starting from $[ReOCl_3(PPh_3)_2]$.[38–40]

A more general procedure for the synthesis of selenolato and tellurolato ligands has recently been published by the *in situ* reduction of diaryldichalcogenides with $LiBH_4$. (Scheme 1). Subsequent reactions with compounds such as $(NBu_4)[TcOCl_4]$ or $[TcCl_3(PPh_3)_2(CH_3CN)]$ gave a number of stable technetium(V) and technetium(III) complexes in clean reactions.[41]

Such an approach can also be applied for the heavier congener of technetium, rhenium. In the present work, we describe the synthesis of a series of rhenium(V) and rhenium(III) complexes with arylselenolato and -tellurolato ligands having different steric demands. The synthesis starts from the corresponding dichalcogenides. as is shown in Scheme 1.

[a] Dr. B. Noschang Cabral, Dr. J. Fonseca Rodrigues, Prof. Dr. E. Schulz Lang
Universidade Federal de Santa Maria
Departamento de Química
97105-900, Santa Maria, Rio Grande do Sul (Brazil)
E-mail: eslang@ufsm.br
https://www.ufsm.br/grupos/lmi

[b] Dr. M. Roca Jungfer, Dr. A. Krebs, Dr. A. Hagenbach, Prof. Dr. U. Abram
Institute of Chemistry and Biochemistry
Freie Universität Berlin
Fabeckstr. 34/36, 14195 Berlin (Germany)
E-mail: ulrich.abram@fu-berlin.de
https://www.bcp.fu-berlin.de/chemie/chemie/forschung/InorgChem/agabram

Supporting information for this article is available on the WWW under https://doi.org/10.1002/ejic.202300023

Research Article
doi.org/10.1002/ejic.202300023



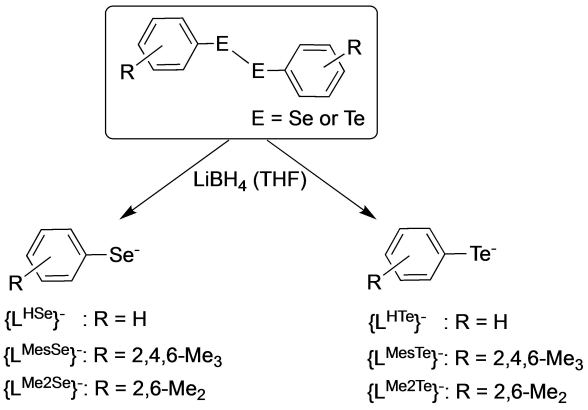


**Scheme 1.** Arylselenolates and -tellurolates used in this study.

## Results and Discussion

Diaryldichalcogenides (Aryl-E–E-Aryl) are yellow (E=Se) or red (E=Te) solids, which can readily be prepared from reactions of Grignard reagents with elemental chalcogens as has been described for the tellurium compounds by *Haller* and *Irgolic*.[42] *In situ* reduction of a slight excess of the corresponding diaryldichalcogenides with $LiBH_4$ in THF solution results in the formation of the reactive lithium arylselenolates Li($L^{RSe}$) and -tellurolates Li($L^{RTe}$) (R=H, 2,4,6-$Me_3$, 2,6-$Me_2$; see Scheme 1), which in turn react with common Re(V) and Re(III) precursors such as [$Re^{V}OCl_3(PPh_3)_2$] or [$Re^{III}Cl_3(PPh_3)_2(CH_3CN)$] with satisfactory yields.

### Oxidorhenium(V) complexes

The structural chemistry of oxidorhenium(V) compounds is well-established and particularly chelating thiolates are perfectly suitable to stabilize the high-valent $\{ReO\}^{3+}$ core. But also stable complexes with monodentate thiophenols are known,[43–49] while only a few examples of ReO complexes with arylselenolato and -tellurolato ligands are found in the literature.[34,35,37–40] Complexes with monodentate phenolato ligands are hitherto unknown. [$ReOCl_3(PPh_3)_2$] proved to be a more favorable starting material than ($NBu_4$)[$ReOCl_4$] for the syntheses of such compounds. Generally, the same products can be prepared starting from tetrachloridooxidorhenate(V) salts, but with significantly lower yields and accompanied with a number of selenium- or tellurium-containing impurities. Similar observations were found for corresponding reactions with a series of selenium- and tellurium-containing Schiff bases, where the released $PPh_3$ plays an active part as reductant, but also as reactive intermediate for the trapping of excess chalcogenides.[38] Interestingly, the described problems do not apply for reactions of the intermediately produced lithium arylchalcogenolates with the corresponding technetium complex ($NBu_4$)[$TcOCl_4$].[41] This effect, however, can be understood by the faster reaction kinetics with the second row transition metal and the rapid precipitation of the products.

The sparingly soluble [$ReOCl_3(PPh_3)_2$] dissolved after addition to a solution of the corresponding lithium chalcogenolates within 30 minutes. The addition of ($NBu_4$)Br resulted in the precipitation of brown (Se compounds) or purple (Te complexes) microcrystals (see Scheme 2). Single crystals suitable for X-ray diffraction were obtained by recrystallization from $CH_2Cl_2$/MeOH (**1**–**3**) or dimethylacetamide (**4**).

Since no structural data of oxidorhenium(V) complexes with monodentate phenols were available for comparison, we synthesized {$Li(THF)_4$}[$ReO(L^{Me2O})_4$] by a reaction of [$ReOCl_3(PPh_3)_2$] with previously isolated Li{$L^{Me2O}$} in THF. The compound crystallizes as THF adduct from the reaction mixture upon cooling to −20 °C as large blue plates, which were suitable for X-ray diffraction. The lithium salt is extremely sensitive against moisture and the crystals immediately decomposed under ambient conditions. The addition of one equivalent of ($AsPh_4$)Cl to the raw reaction mixture, however, gave a blue powder of the more stable tetraphenylarsonium salt.

The products are five-coordinate with the oxido ligands at the apexes of square pyramids. The Re=O bonds are in the usual range between 1.63 and 1.70 Å. Expectedly, the O1–Re–Se/Te/O angles are clearly larger than 90°, which brings the rhenium atoms in positions approximately 0.7–0.8 Å above the basal planes formed by the four chalcogen atoms. Since the structures of the compounds are very similar, only those of the [$ReO(L^{HSe})_4]^-$, [$ReO(L^{MesTe})_4]^-$ and [$ReO(L^{Me2O})_4]^-$ complex anions are shown in Figure 1. Selected bond lengths and angles are summarized in Table 1. The Re–Se and Re–Te bonds are in the ranges observed for oxidorhenium(V) complexes with the chalcogenolato-substituted Schiff bases in Ref. [38]. The aromatic rings are twisted by approximately 90° against the planes formed by the chalcogen atoms in all complexes under study (Figure 1).

The $\nu_{ReO}$ stretches of the ($NBu_4$)[$ReO(L^{RSe/Te})_4$] complexes are found as bands between 960 and 980 $cm^{-1}$ in the IR spectra of the compounds. This is the common region for five-coordinate

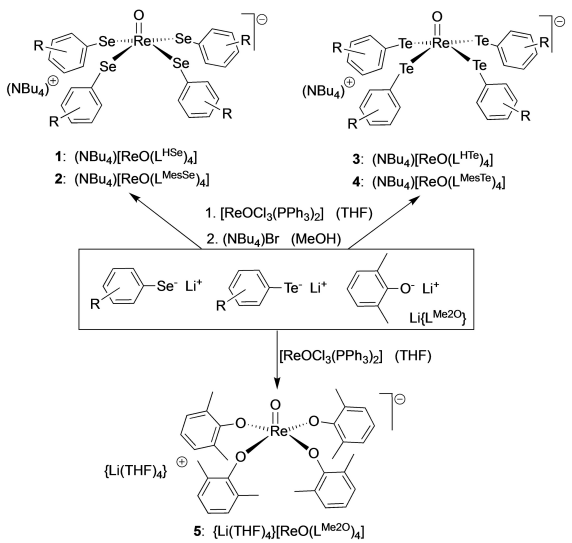


**Scheme 2.** Syntheses of the oxidorhenium(V) complexes.

Research Article
doi.org/10.1002/ejic.202300023



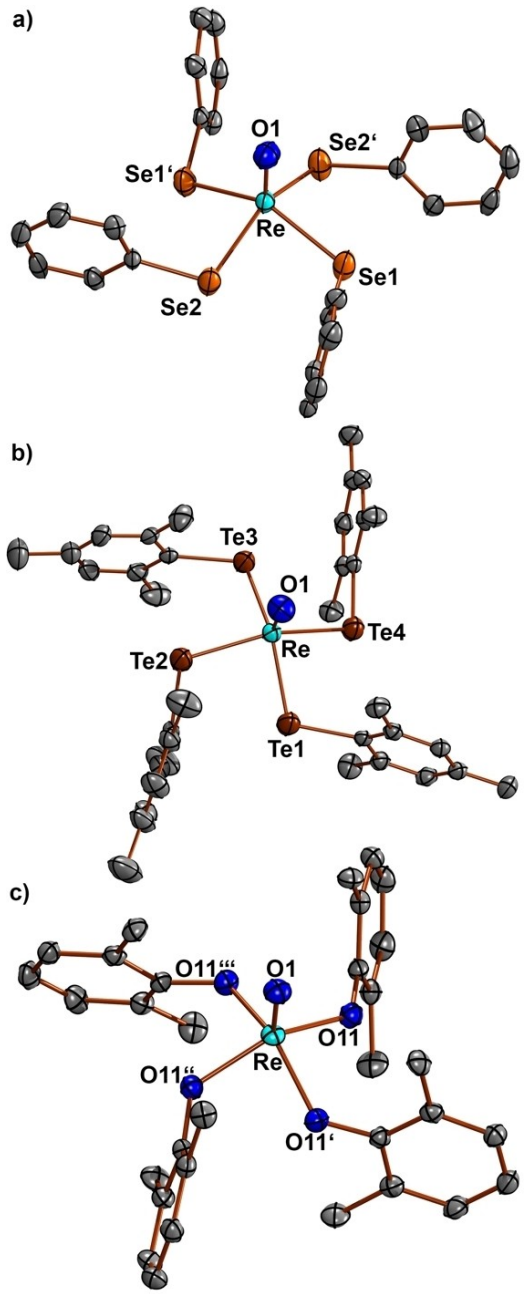


**Figure 1.** Structures of the oxidorhenium(V) complexes a) $[ReO(L^{HSe})_4]^-$ (**1**), b) $[ReO(L^{MesTe})_4]^-$ (**4**) and c) $[ReO(L^{Me2O})_4]^-$ (**5**). Ellipsoids are depicted at 50% probability. For clarity, the $NBu_4^+$ cations, co-crystallized solvent molecules and hydrogen atoms are omitted. Symmetry operations for a) (') −x, y, $^1/_2$−z. Symmetry operations for c) (') y,0.5−x,z; ('') 0.5−x,0.5−y,z; (''') 0.5−y,x,z.

oxidorhenium(V) compounds,[1] and also the analogous technetium complexes show $\nu_{TcO}$ frequencies in the same range.[41] Expectedly, the square pyramidal $d^2$ complexes under study are diamagnetic and give well resolved $^1$H and $^{13}$C NMR spectra. The detection of three resolved methyl signals for the methyl groups in the $[ReO(L^{MesSe})_4]^-$ and $[ReO(L^{MesTe})_4]^-$ anions in compounds **2** and **4** confirm that the twisted conformation of the ligands found in the solid state structures (with one of the methyl groups in *syn*- and one in *anti*-position to the Re=O bond, see Figure 1b) is maintained in solution. The $^{77}$Se NMR signals of **1** and **3** appear at 462.9 and 368.1 ppm, respectively. This in the range found for other transition metal selenolato complexes.[41,50] The same is observed for the corresponding tellurium compounds, where $^{125}$Te chemical shifts of 462.9 and 286 ppm are observed for complexes **2** and **4**. The first value is practically identical with that of $(NBu_4)[TcO(L^{HTe})_4]$.[41] $^{77}$Se/$^{125}$Te NMR spectroscopy is suitable to assess the stability of the complexes in solution. While the selenium compounds are stable for several hours in solution, a subsequent decomposition of the tellurium complexes **2** and **4** is observed, which goes along with the reformation of the corresponding diaryldditellurides and the appearance of their $^{125}$Te NMR signals at 417.6 and 193.2 ppm, respectively. Negative mode ESI TOF mass spectra show intense signals for the molecular peaks of the respective molecular anions. Fragmentation mainly occurs by the release of complete ligands.

### Rhenium(III) complexes

$[ReCl_3(PPh_3)_2(CH_3CN)]$ is a common starting material for the synthesis of low-valent rhenium complexes. It can conveniently be prepared from $[ReOCl_3(PPh_3)_2]$ and $PPh_3$ in acetonitrile and readily reacts with a large variety of ligand systems under formation of five- or six-coordinate rhenium(III) compounds.[1,51]

Reactions between the *in situ* prepared lithium arylchalcogenolates and $[ReCl_3(PPh_3)_2(CH_3CN)]$ or the analogous $[ReCl_3(PMe_2Ph)_3]$ give five-coordinate Re(III) complexes. The products are purple (Se compounds) or brown (Te compounds) solids, which precipitate from the reaction mixtures. Their individual compositions are summarized in Scheme 3.

All products show a trigonal bipyramidal coordination environment for the rhenium atoms. The three aryl chalcogenolates are placed in the trigonal plane, while the axial positions are occupied by a combination of a $PPh_3$ and an acetonitrile ligand (compounds **6**, **7** and **9**) or two phosphine ligands (compounds **8** and **10**). Exemplarily, the molecular structures of $[Re(PPh_3)(CH_3CN)(L^{HSe})_3]$ (**6**) and $[Re(PPh_3)_2(L^{HTe})_3]$ (**8**) are shown in Figure 2. Ellipsoid plots of the other complexes are depicted in the Supporting Information. At this place, also more detailed lists of bond lengths and angles for all complexes can be found, while Table 2 contains only a brief comparison of relevant

**Table 1.** Selected bond lengths (Å) and angles (°) for the $[ReO(L^{RSe/Te})_4]^-$ anions and $[ReO(L^{Me2O})_4]^-$.

| | 1 | 2 | 3 | 4 | 5 |
|---|---|---|---|---|---|
| Re–O1 | 1.682(6) | 1.700(3) | 1.667(7) | 1.687(6) | 1.670(5) |
| Re–E | 2.469(1)–2.473(1) | 2.458(1)–2.480(1) | 2.653(1)–2.661(1) | 2.621(1)–2.663(1) | 1.967(2) |
| O1–Re–E | 108.04(2)–108.67(2) | 105.6(1)–109.9(1) | 107.01(1)–109.08(1) | 105.7(2)–107.6(2) | 108.38(7) |

Research Article
doi.org/10.1002/ejic.202300023



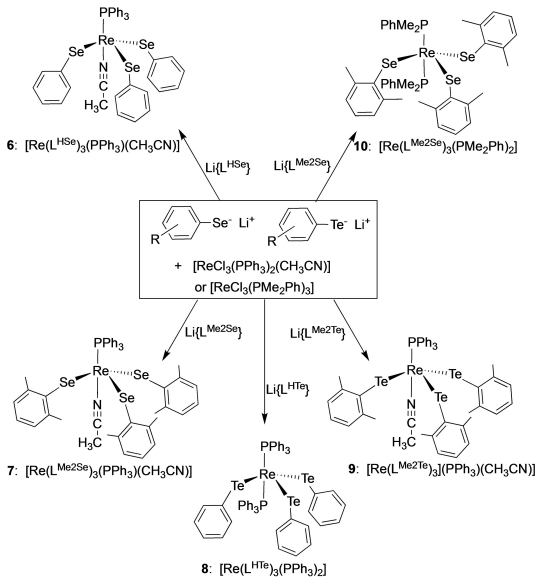


**Scheme 3.** Syntheses of five-coordinate rhenium(III) complexes.

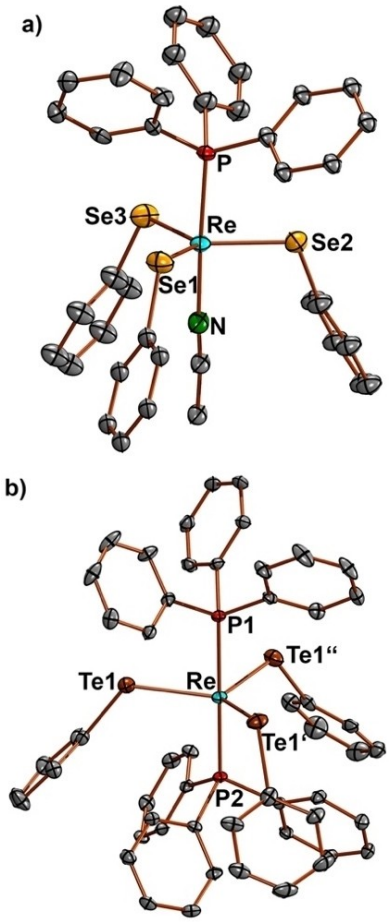


**Figure 2.** Molecular structures of complexes a) **6** and b) **8**. Ellipsoids are depicted at 50% probability. Hydrogen atoms and solvate molecules were omitted for clarity. Symmetry operations: (') 1−y, x−y, z, (") 1−x+y, 1−x, z.

bonding parameters of the $[Re(PPh_3)(CH_3CN)(L^{RSe/Te})_3]$ complexes **6**, **7** and **9** and $[Re(PPh_3)_2(L^{HTe})_3]$ (**8**).

It is particularly interesting to note that in the complex with unsubstituted phenyltellurolate, $[Re(PPh_3)_2(L^{HTe})_3]$ (**8**), two triphenylphosphine ligands find space in the axial positions. The experimental results strongly suggest that the composition of the final products of such reactions are influenced both by electronic (preference of phosphines whenever possible) and steric factors (size of the phosphines). The coordination of two axial phosphine ligands is preferred as long as this is not precluded by the steric bulk of the phosphines or the chalcogenolates. The structural flexibility of the products is impressively demonstrated for compound **8**, where the coordination of two $PPh_3$ ligands becomes possible by the formation of remarkably long Re–P bonds. With 2.442(2) Å, they are longer by approximately 0.1 Å than the values in complexes **6**, **7** or **9**. This allows P1–Re–Te angles as small as 83.961(7)°. The Re–Te–C angles of around 120° are clearly larger than the values in the other Re(III) complexes under study. Both effects open the cone angle for the coordination of a second $PPh_3$ ligand, which (also supported by the long Re–Te bonds) is surrounded by an umbrella-like arrangement of the three phenyl rings of the tellurolate. Figure 3 represents space-filling models of the complexes **6**–**9** in a projection along the trigonal axes. For a better illustration of the space, which is available for the coordination of the second axial ligand ($CH_3CN$ in the case of compounds **6**, **7** and **9**, and $PPh_3$ in the case of complex **8**) by the discussed difference in the Re–Se/Te bond lengths and the Re–Se/Te–C angles, these ligands have been removed from the molecules.

It becomes evident that the available space in complexes **6**, **7**, and **9** is well suitable for the coordination of a linear ligand such as acetonitrile, but not for the bulkier $PPh_3$. The restrictions in the selenium-containing complexes may be mainly due to the relatively short Re–Se bonds, but it is interesting to note

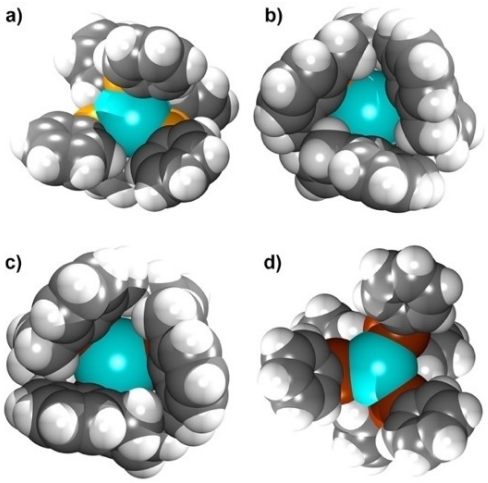


**Figure 3.** Space-filling models of (a) $[Re(PPh_3)(CH_3CN)(L^{HSe})_3]$ (**6**), b) $[Re(PPh_3)(CH_3CN)(L^{Me2Se})_3]$ (**7**), c) $[Re(PPh_3)(CH_3CN)(L^{HTe})_3]$ (**9**) and d) $[Re(PPh_3)_2(L^{HSe})_3]$ (**8**) after the removal of the second axial ligands ($CH_3CN$ or $PPh_3$) illustrating the space available for coordination in *trans*-position to the phosphorus atom P1 (see Figure 2).

Research Article
doi.org/10.1002/ejic.202300023


**Table 2.** Selected bond lengths (Å) and angles (°) for the rhenium(III) complexes.

| | 6 | 7 | 8 | 9 |
|---|---|---|---|---|
| Re–P1 | 2.357(4) | 2.333(2) | 2.442(2) | 2.340(1) |
| Re–N/P2 | 2.08(1) | 2.084(7) | 2.386(2) | 2.074(5) |
| Re–Se/Te | 2.373(2)–2.380(2) | 2.3782(8)–2.3904(8) | 2.5836(3) | 2.5474(4)–2.5671(5) |
| P1–Re–N/P2 | 177.0(4) | 177.0(2) | 180 | 177.8(1) |
| P1–Re–Se/Te | 86.8(1)–89.4(1) | 88.20(5)–89.62(5) | 83.961(7) | 89.14(4)–90.29(4) |
| Re–Se/Te–C | 110.4(6)–114.8(6) | 108.1(2)–109.8(2) | 119.8(1) | 105.2(2)–106.8(2) |

that also for the complexes with the bulkier $\{L^{Me2Se/Te}\}^-$ ligands the 'umbrella-like' conformation with all three chalcogenolates pointing to the same side of the trigonal plane is found.

Another arrangement of the ligands, however, is found for the product of a similar reaction of $Li\{L^{Me2Se}\}$ with $[ReCl_3(PMe_2Ph)_3]$: $[Re(PMe_2Ph)_2(L^{Me2Se})_3]$ (**10**). The structure of the complex with the sterically less restricting $PMe_2Ph$ is shown in Figure 4. Also here, the Re–P bonds are clearly longer than in the $[Re(PPh_3)(CH_3CN)(L^{RSe/Te})_3]$ complexes. Due to the steric bulk of the 2,6-dimethyl substitution of the phenylselenolato ligands they cannot establish the umbrella-like conformation found in the other complexes (including compound **8**). Similar findings are reported for trigonal bipyramidal thiolato complexes of rhenium(III), technetium(III), molybdenum(II) or tungsten(II) with carbonyl ligands, for which different arrangements of the thiolato ligands were observed.[52–54]

As in the related technetium thiolato complexes of the composition $[Tc(NCCH_3)_2(arylthiolates)_3]$,[54] the disposition of the chalcogenolate rings in compound **10** persists dissolution. Three signals for the methyl groups are visible in the $^1H$ NMR spectrum of the compound and its $^{77}Se$ NMR spectrum shows two signals at 920.1 and 933.4 ppm.

The observed $^{77}Se$ and $^{125}Te$ NMR signals of Re(III) complexes indicate an effective deshielding of the chalcogen nuclei in comparison with the oxidorhenium(V) complexes discussed above. This suggests effective Re–Se/Te interactions (σ- and π-donation), which is finally also confirmed by the markedly shorter rhenium-chalcogen bonds in the Re(III) compounds.

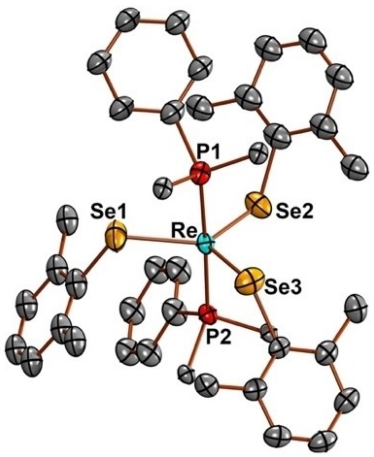


**Figure 4.** Molecular structure of complex **10**. Ellipsoids are depicted at 50% probability. Hydrogen atoms have been omitted for clarity. Re–P1 2.442(2), Re–P2 2.405(2), Re–Se 2.3648(7)–2.3835(7) Å; P1–Re–P2 177.71(5), P1–Re–Se1 82.97(4), P1–Re–Se3 82.03(4), P1–Re–Se2 97.87(4), Re–Se–C 116.9(2)–119.8(2)°.

## Computational Studies

There is hitherto no systematic study about the nature of rhenium-chalcogen bonds for rhenium(V) compounds due to the lack of an isostructural series of crystallographically characterized compounds to support the computational results. Therefore, we performed some DFT calculations on the B3LYP level for $[ReO(L^{HE})_4]^-$ ions with E=O, S, Se and Te. The experimental data for the thiophenolato complex are taken from Ref. [45].

The trends of the bond parameters of the crystal structures are also well resembled in the optimized structures. Details about the resulting parameters and a comparison with the experimental data are given as Supporting Information. The variation of the four chalcogen donors does not significantly influence the rhenium-oxygen double bonds. The Re–E–C angles decrease from O to Te with a marked step from oxygen to sulfur. In contrast to the other chalcogen atoms, the oxygen atom has markedly more $sp^2$ character and, thus, the angle is close to the trigonal 120°. From sulfur to tellurium the chalcogen atom s-character in the hybridization gradually decreases, which results in an "$sp^3$ situation" at tellurium with an almost tetrahedral bond angle of 108°.

The decomposition of the atomic orbital contribution of the NBO analysis clearly shows a decrease in s character and a gain of p character in the hybrid orbitals from O (29% s, 70% p) to Te (17% s, 83% p). Again, the most drastic changes are observed when going from O to S (29% s to 20%, 70% p to 79%), see Supporting Information. Furthermore, the d-orbital contribution of the rhenium decreases substantially from O to Te. Also here, the most drastic change is observed from O to S (94% d to 39% d) followed by a steady trend to Te, where the p character slowly increases while the d character decreases. Furthermore, the number of electrons localized in bonding (Lewis) orbitals decreases, which means that due to delocalization some of the electrons are partially localized in non-Lewis orbitals in the ground state resulting in non-integer numbers of electrons. This accessibility of non-Lewis orbitals and, thus, the delocalization increase from O to Te with the most drastic change from O to S (99.8% Lewis to 94.0). The character of the

Research Article
doi.org/10.1002/ejic.202300023


Re=O bond is not affected by the nature of the chalcogen atom.

As a check of covalency in the bonds, Baders quantum theory of atoms in molecules (QTAIM) was applied and the electron density in the respective basins was integrated for charge analysis. NBO and Mulliken charges were additionally calculated. The ionicity of the rhenium-chalcogen bonds decreases according to the Bader charge model from O to Te as the charge differences between Re and the chalcogen decrease. For both the NBO and the Mulliken charges an inversion of the normal charge situation ($Re^{+}$–$E^{-}$) to $Re^{-}$–$E^{+}$ (NBO: E=S, Se, Te; Mulliken: E=Te) is implicated by the results of the calculations. This is uncommon but not unknown, since similar results were obtained for the analogous technetium complexes.[41] In both the Mulliken and Bader charges the rhenium has a low positive or low negative charge but still a more positive charge than the oxido ligand. Furthermore, the charge of the oxido ligand in the Bader model decreases drastically from O to S but increases from S to Te (see Supporting Information). Overall, the Bader model yields the most realistic description of the charge situation for the present compounds.

The Wiberg bond orders of the compounds reveal an increase of the triple bond character of the Re–O1 bond from O to Te (for the individual data see the Supporting Information). Remarkably, the bond order first decreases from O to S and then increases from S via Se to Te. The bond order of the rhenium-chalcogen bond increases from O to Te with the most drastic increase from O to S. The inversely proportional carbon-chalcogen bond order, which is highest for O, reveals some double bond character in the phenolato ligands compared to the other three chalcogens. Interestingly, the heavier chalcogens show some inter-chalcogen interactions which is illustrated by the increase in the bond order. This interaction is formed between the chalcogen atoms in the equatorial coordination plane, and additionally to the oxido ligand at the rhenium.

According to the calculated electron localization functions (ELFs), the bonds between the rhenium and the chalcogen atoms get more delocalized in the series under study when going from the phenolato to the tellurolato complexes. The calculated bond character is, thus, for the heavier chalcogens in agreement with the concept of a more metallic bond. The ELF surface cutting the rhenium-chalcogen-chalcogen plane also reveals that there is increasing overlap of the rhenium $d_{x^2-y^2}$ with two neighboring (*cis*) chalcogen p orbitals from sulfur to tellurium indicating a marked metallic character for these bonds. In contrast, no such interactions of the oxygen atoms of the phenolato complex are observed. This supports the findings discussed for the bond orders: a higher degree of delocalization is present in the heavier chalcogen structures. The increase of the chalcogen p-orbital and core size is also visible in the ELF plots (see Figure 5 and Supporting Information).

The gradient field Bader basin analyses of the complexes slightly above the equatorial planes formed by the chalcogen atoms reveal that the electron density around the metal is more localized for the phenolato complex and, thus, less evenly distributed around Re than for the other chacogenolato

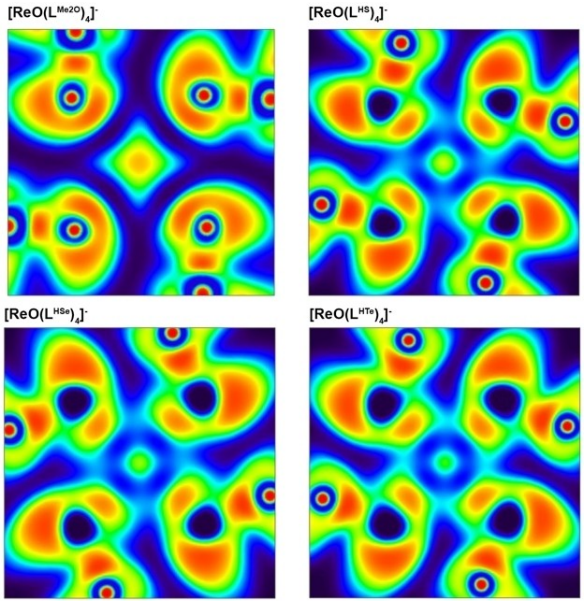


**Figure 5.** Electron localization function (ELFs) of the oxidorhenium(V) complexes in the $E_4$ planes of the complexes (E=O, S, Se, Te).

complexes. It decreases, however, up to an ideal delocalization for the tellurolato complex. Therefore, the part of the bonds localized at the rhenium atom in phenolato complex **5** is more localized or directional than in the complexes with the heavier chalcogens. In contrast, the field gradients surrounding the chalcogen atoms show that the phenolato oxygen atoms of complex **5** have more evenly distributed electron density than the more directional gradients surrounding the heavier chalcogen atoms. In conclusion, the rhenium-chalcogen bonds are more ionic, localized or directional for the phenolato complex at the rhenium atom and more delocalized at the oxygen atoms, while the opposite is observed in the complexes with the heavier chalcogenolates, where the chalcogen orbitals are directional but allow for a consistent, metallic network of electron flux around the rhenium atoms. The rhenium atoms participate in the delocalization not only with the bonding orbitals but also with the $d_{x^2-z^2}$, which fills the space between the chalcogen orbitals. The points of the zero-flux surfaces are shown in Figure 6 in different colors resembling their character. Saddle points are shown in grey, maxima and chalcogen atoms in black and the respective central rhenium atom in yellow. The gradient electron density field is resembled by blue lines while the basin boundaries are shown as black lines.

In contrast to the situation in the oxidorhenium(V) compounds, where the electronic charges around the rhenium atoms are more homogeneously distributed (Figures 5 and 6), that in the Re(III) compounds reveals a more directional character with the charge being located along the lines connecting the Re and Se/Te atoms. From the derived parameters (see Supporting Information) it can be stated that the ellipticity of the electron density decreases along the group as the double-bond ($\pi$) character of the Re–E bond decreases for the heavier chalcogens. Contrastingly, the bond strength

Research Article
doi.org/10.1002/ejic.202300023


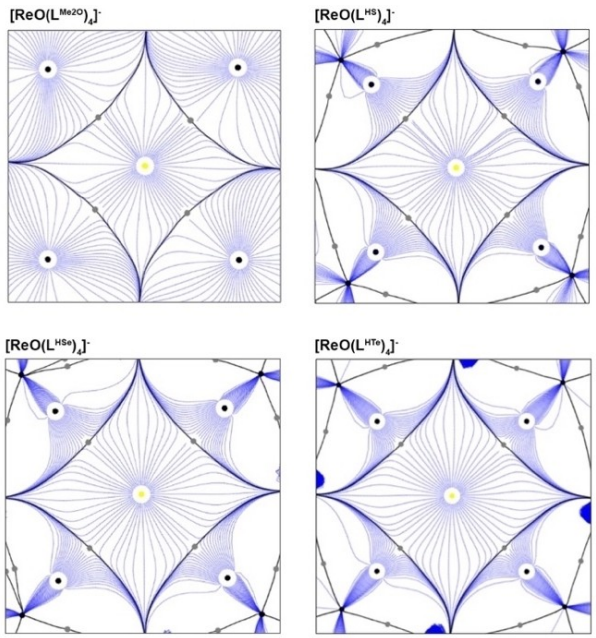


**Figure 6.** Gradient-field Bader basin analysis of the oxidorhenium(V) complexes slightly above the $E_4$ planes of the complexes (E=O, S, Se, Te).

between rhenium and the chalcogen atom decreases from sulfur to tellurium, but increases from Re(III) to Re(V).

Similarly, the metallicity of the Re–E bonds decreases from tellurium to sulfur and increases from Re(V) to Re(III). The corresponding metallicity values, however, while being close to a value of 1 for the rhenium tellurolato complexes do not seriously support true metallic interactions. The only two exceptions are the hypothetical complexes [Re(TePh)$_3$(PPh$_3$)(CH$_3$CN)] and [Re(TePhMe$_2$)$_3$(PPh$_3$)$_2$]. Both compounds could not be isolated as products of the reaction between [ReCl$_3$(PPh$_3$)$_2$(CH$_3$CN)] and the corresponding tellurolates where [Re(TePh)$_3$(PPh$_3$)$_2$] (**8**) and [Re(TePhMe$_2$)$_3$(PPh$_3$)(CH$_3$CN)] (**9**) were the sole products.

Some differences between the electronic structures of [Re(TePh)$_3$(PPh$_3$)$_2$] (**8**) and the hypothetical [Re(TePh)$_3$(PPh$_3$)(CH$_3$CN)] as well as [Re(TePhMe$_2$)$_3$(PPh$_3$)(CH$_3$CN)] (**9**) and its hypothetical counterfeit [Re(TePhMe$_2$)$_3$(PPh$_3$)$_2$] can be derived from the NBO analyses of the complexes: **8** and **9**, as all other experimentally accessible compounds, show higher-lying rhenium d-orbitals and lower-lying tellurium p-orbitals than their hypothetical counterparts. The electronic differences between the two pairs of compounds become obvious when looking at the ELF plots (Figure 7), which suggest that a more even distribution of electrons around the chalcogen atom may be favourable.

The second order perturbation interaction energies of the NBO analysis between additional chalcogen p orbitals and rhenium d orbitals suggest that the most stable structures minimize the π-donation by the heavier chalcogen atoms, again

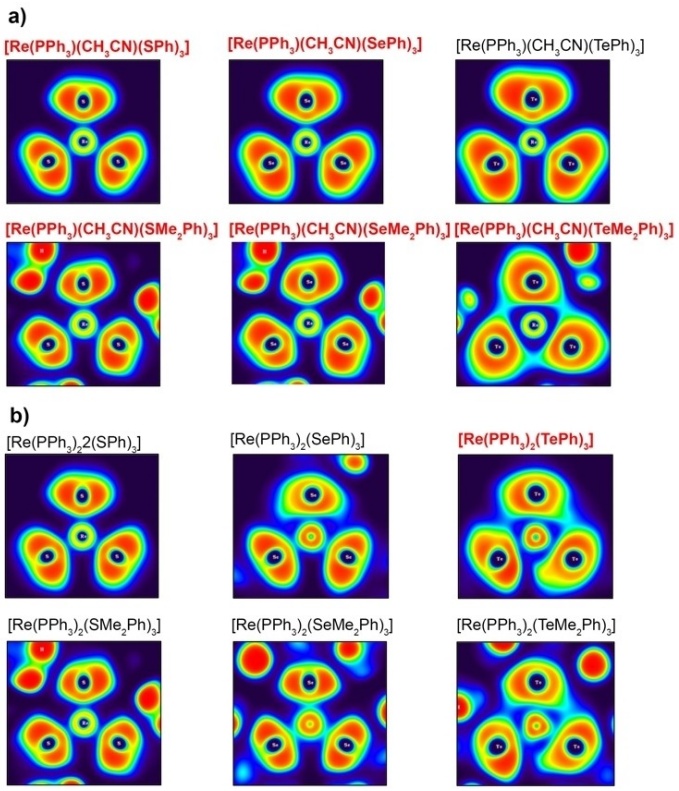


**Figure 7.** ELF plots for the trigonal coordination spheres of the a) [Re(EAr)$_3$(PPh$_3$)(CH$_3$CN)] and b) [Re(EAr)$_3$(PPh$_3$)$_2$] complexes (E=S, Se, Te). Isolated compounds are highlighted in red.

supporting electronic reasons for the formation of [Re(TePh)$_3$(PPh$_3$)$_2$] (**8**) and [Re(TePhMe$_2$)$_3$(PPh$_3$)(CH$_3$CN)] (**9**) instead of their CH$_3$CN or PPh$_3$ analogues respectively.

## Conclusion

Square pyramidal oxidorhenium(V) and trigonal bipyramidal rhenium(III) complexes with monodentate arylselenolato or aryltellurolato ligands can be prepared in simple procedures starting from [ReOCl$_3$(PPh$_3$)$_2$] or [ReCl$_3$(PPh$_3$)$_2$(CH$_3$CN)] and *in situ* generated lithium chalcogenolates. The products are stable as solids, but gradually decompose in solution under release of the chalcogenolates and re-formation of the corresponding diaryldiselenolates and -tellurolates.

DFT calculations show that on a series of [ReO(EAryl)$_4$]$^-$ complexes (E=O, S, Se, Te) the rhenium-chalcogen bonds are significantly more ionic and localized for the phenolato complex compared with the heavier chalcogens. Generally, the Re–Se and Re–Te bonds are more directional in the Re(III) complexes than in the oxidorhenium(V) compounds.

## Experimental Section

All chemicals were reagent grade and used without further purification. Solvents were dried and used freshly distilled unless otherwise stated. [ReOCl$_3$(PPh$_3$)$_2$], [ReCl$_3$(PPh$_3$)$_2$(CH$_3$CN)] and [ReCl$_3$(PMe$_2$Ph)$_3$] were prepared according to published procedures.[55–57] The diaryl dichalcogenides were synthesized following the general procedure of Irgolic et al.[42]

Infrared spectra were measured as KBr pellets on a Bruker Vector 22 FTIR-spectrometer between 400 and 4000 cm$^{-1}$. NMR spectra were recorded on a Bruker Advance III HD 600 MHz spectrometer or on a Jeol ECX/400 400 MHz spectrometer. ESI mass spectra were measured with an Agilent 6210 ESI TOF mass spectrometer (Agilent Technologies). All MS results are given in the form: m/z assignment. Elemental analyses of carbon, hydrogen and nitrogen were performed using a Heraeus Vario EL elemental analyzer. Some of the analyses unfortunately show unsatisfactory deviations (particularly for the carbon values). This is frequently observed for rhenium complexes. Too low values are commonly attributed to an incomplete combustion. We provided the best values we obtained for the compounds to date.

### Crystallography

The intensities for the X-ray determinations were collected with Mo Kα radiation (λ = 0.71073 Å) on a D8 Venture Bruker instrument (compounds **2**, **4**, **8** and **10**) or a STOE IPDS (compounds **1**, **2**, **5**, **6**, **7** and **9**). Standard procedures were applied for data reduction and absorption correction. Structure solution and refinement were performed with the SHELX program package using the OLEX2 platform.[58,59] Hydrogen atoms were calculated for idealized positions and treated with the 'riding model' option of SHELXL. Electron density belonging to highly disordered solvent molecules have been removed by the BYPASS option of OLEX2 during the refinement of the crystal structures of (NBu$_4$)[ReO(L$^{MesTe}$)$_4$] (**4**) (one molecule of dimethyl acetamide) and [Re(PPh$_3$)$_2$(L$^{HTe}$)$_3$]·(**8**) (0.3 molecule of CHCl$_3$). Graphic representations of the complexes were done with the DIAMOND software.[60]

Deposition Numbers 2182902 (for **1**), 2182907 (for **2**), 2182903 (for **3**), 2182908 (for **4**), 2232200 (for **5**), 2182909 (for **6**), 2182918 (for **7**), 2183044 (for **8**), CCDC 2182919 (for **9**), 2182920 (for **10**) contain the supplementary crystallographic data for this paper. These data are provided free of charge by the joint Cambridge Crystallographic Data Centre and Fachinformationszentrum Karlsruhe Access Structures service.

### Syntheses

*(NBu$_4$)[ReO(L$^{RSe}$)$_4$] complexes:* The diaryldiselenide (0.25 mmol; {L$^{HSe}$}$_2$: 78 mg, {L$^{MesSe}$}$_2$: 99 mg) was dissolved in 3 mL of a CHCl$_3$/MeOH mixture (1:2, v/v) and a 2 M solution of LiBH$_4$ in THF (0.25 mL, 0.5 mmol) was added dropwise in an atmosphere of dry argon. The reduction was completed when the yellow color of the diaryldiselenide disappeared and a colorless solution was formed. Solid [ReOCl$_3$(PPh$_3$)$_2$] (83 mg; 0.1 mmol) was added to the solution. The sparingly soluble solid dissolved within 30 min. The remaining dark brown solution was filtered and (NBu$_4$)Br (32 mg, 0.1 mmol) dissolved in 1 mL of MeOH was added. Immediately, a brown precipitate of the corresponding (NBu$_4$)[ReO(L$^{RSe}$)$_4$] complex was formed, which was filtered off, washed with MeOH (2 mL) and dried under vacuum.

(NBu$_4$)[ReO(L$^{HSe}$)$_4$] (**1**): Yield: 69 % (74 mg), Brown crystals, recrystallization from CH$_2$Cl$_2$/MeOH (1:1, v/v). Elemental analysis: Calcd for C$_{40}$H$_{56}$NOReSe$_4$: C, 44.9, H; 5.3; N, 1.3 %. Found: C, 45.4; H, 5.3; N, 1.4 %. IR (KBr, cm$^{-1}$): 3053 (w), 2956 (m), 2872 (w), 1571 (m), 1471 (s), 1379 (w), 1020 (m), 960 (s), 736 (s), 629 (s), 474 (s). ESI- MS (m/z): 826.7802 [M]$^-$ (calcd. 826.7748). $^1$H NMR (600 MHz, DMSO-d$_6$) δ (ppm): 7.51–7.54 (m, 8H), 7.16–7.21 (m, 8H), 7.10–7.15 (m, 4H), 3.09–3.16 (m, 8H), 1.54 (quint, *J* = 7.8 Hz, 8H), 1.30 (h, *J* = 7.4 Hz, 8H), 0.93 (t, J = 7.3 Hz, 12H). $^{13}$C{$^1$H} NMR (150 MHz, DMSO-d$_6$) δ (ppm): 138.4, 136.6, 127.4, 125.7, 57.4, 22.9, 19.1, 13.4. $^{77}$Se NMR (114 MHz, DMSO-d$_6$) δ (ppm): 462.9.

(NBu$_4$)[ReO(L$^{MesSe}$)$_4$] (**2**): Yield: 70 % (86 mg). Brown solid, recrystallization from CH$_2$Cl$_2$/MeOH (1:1, v/v). Elemental analysis: Calcd for C$_{52}$H$_{80}$NOReSe$_4$: C, 50.5; H, 6.5; N, 1.1 %. Found: C, 49.6; H, 6.4; N, 0.9 %. IR (KBr, cm$^{-1}$): 3011 (w), 2963 (s), 2876 (m), 1597 (w), 1459 (s), 1459 (m), 1035 (m), 961 (s), 847 (m), 737 (w), 548 (w). ESI- MS (m/z): 994.9641 [M]$^-$ (calcd. 994.9626). $^1$H NMR (600 MHz, CD$_2$Cl$_2$) δ (ppm): 6.90 (s, 8H), 2.79–2.83 (m, 8H), 2.50 (s, 12H), 2.31 (s, 12H), 2.27 (s, 12H), 1.35–1.47 (m, 16H), 1.05 (t, *J* = 7.1 Hz, 12H). $^{13}$C{$^1$H} NMR (150 MHz, CD$_2$Cl$_2$) δ (ppm): 145.6, 144.2, 136.8, 135.1, 127.4, 58.6, 24.4, 23.7, 20.8, 19.7, 13.4. $^{77}$Se NMR (114 MHz, CD$_2$Cl$_2$) δ (ppm): 368.1.

*(NBu$_4$)[ReO(L$^{Te}$)$_4$] complexes:* The diaryldittelluride (0.25 mmol; {L$^{HTe}$}$_2$: 102 mg, {L$^{MesTe}$}$_2$: 123 mg) was dissolved in 3 mL of a CHCl$_3$/MeOH mixture (1:2, v/v) and a 2 M solution of LiBH$_4$ in THF (0.25 mL, 0.5 mmol) was added dropwise in na atmosphere of dry argon. The reduction was completed when the red color of the diaryldittelluride disappeared and a colorless solution was formed. Solid [ReOCl$_3$(PPh$_3$)$_2$] (83 mg; 0.1 mmol) was added to the solution. The sparingly soluble solid dissolved within 30 min. The remaining dark (almost black) solution was filtered and (NBu$_4$)Br (32 mg, 0.1 mmol) dissolved in 1 mL of MeOH was added. Immediately, a dark purple precipitate of the corresponding (NBu$_4$)[ReO(L$^{RTe}$)$_4$] complex was formed, which was filtered off, washed with MeOH (2 mL) and dried under vacuum.

(NBu$_4$)[ReO(L$^{HTe}$)$_4$] (**3**): Yield: 53.8 % (68 mg), purple solid. Elemental analysis: Calcd. for C$_{40}$H$_{56}$NOReTe$_4$: C, 38.0; H, 4.5; N, 1.1 %. Found: C, 38.0; H, 4.6; N, 1.1 %. IR (KBr, cm$^{-1}$): 3059 (w), 2956 (s), 2872 (m), 1570 (w), 1469 (s), 1431(m), 1016 (m), 968 (m), 736 (s), 456 (s). ESI–MS (m/z): 1022.7205 [M]$^-$ (calcd. 1022.7256). $^1$H NMR (600 MHz, CD$_2$Cl$_2$) δ (ppm): 7.90–7.93 (m, 4H), 7.84–7.86 (m, 4H), 7.18–7.30 (m,

12H), 3.07–3.13 (m, 8H), 1.59–1.65 (m, 8H), 1.45 (h, $J=7.4$ Hz, 8H), 1.06 (t, $J=7.3$ Hz, 12H). $^{13}C\{^1H\}$ NMR (150 MHz, $CD_2Cl_2$) δ (ppm): 141.7, 137.5, 129.2, 125.6, 58.9, 23.8, 19.7, 13.3. $^{125}Te$ NMR (189 MHz, $CD_2Cl_2$) δ (ppm): 493.7, 417.6 ($Ph_2Te_2$).

$(NBu_4)[ReO(L^{MesTe})_4]$ (**4**): Yield: 63 % (90 mg), purple solid. Elemental analysis: Calcd. for $C_{52}H_{80}NOReTe_4$: C, 43.6; H, 5.6; N, 1.0 %. Found: C, 41.9; H, 6.0; N, 1.0 %. IR (KBr, $cm^{-1}$): 3011 (w), 2963 (s), 2876 (m), 1597 (w), 1459 (s), 1459(m), 1035 (m), 961 (s), 847 (m), 737 (w), 548 (w). ESI- MS (m/z): 1190.9173 $[M]^-$ (calcd. 1190.9134). $^1H$ NMR (400 MHz, DMSO-$d_6$) δ (ppm): 6.81 (s, 8H), 3.11 (t, $J=8.2$ Hz, 8H), 2.47 (s, 12H), 2.26 (s, 12H), 2.20 (s, 12H), 1.52 (quint, $J=8.0$ Hz, 8H), 1.28 (h, $J=7.3$ Hz, 8H), 0.91 (t, $J=7.3$ Hz, 12H). $^{13}C\{^1H\}$ NMR (100 MHz, DMSO-$d_6$) δ (ppm): 145.7, 136.3, 127.3, 122.9, 58.1, 30.1, 29.2, 23.6, 21.1, 19.7, 14.0. $^{125}Te$ NMR (189 MHz, DMSO-$d_6$) δ (ppm): 286.8, 193.2 ($Mes_2Te_2$).

*{Li(THF)$_4$}[ReO(L$^{Me2O}$)$_4$] (**5**) and (AsPh$_4$)[ReO(L$^{Me2O}$)$_4$] (**5 a**)*: $Li(L^{Me2O})$ (231 mg, 3 mmol) was dissolved in absolutely dry THF under an atmosphere of dry argon and carefully dried $[ReOCl_3(PPh_3)_2]$ (500 mg, 0.6 mmol) was added. The mixture was stirred at room temperature for approximately 90 min. The solid rhenium starting material slowly dissolved and finally a clear blue solution was obtained. Concentration of the reaction mixture in vacuum gave deep blue, highly sensitive crystals of a THF adduct of the lithium salt **5**, from which a single crystal structure could be measured. All attempts to isolated the compound as a pure solid failed, since the crystals immediately decompose under loss of the incorporated solvent under formation of a dark, intractable oil. A solid product, however, could be obtained after the addition of $(AsPh_4)Cl$ to the reaction mixture and subsequent concentration. The formed $(AsPh_4)[ReO(L^{Me2O})_4]$ (**5 a**) can be isolated as a bluish powder. Yield on **5 a**: 50 %. IR (KBr, $cm^{-1}$): 3063 (w), 2963 (w), 1434 (m), 1260 (m), 1080 (m), 1022 (w), 984 (m), 906 (m), 741 (m), 693 (m), 481 (m). $^1H$ NMR (400 MHz, $CDCl_3$) δ (ppm): 6.96 (d, 2H), 6.73 (t, 1H), 4.75 (s, 1H), 2.24 (s, 3H).

*Rhenium(III) triphenylphosphine complexes*: The diaryldichalcogenide (0.2 mmol; $\{L^{HSe}\}_2$: 62 mg, $\{L^{Me2Se}\}_2$: 74 mg, $\{L^{HTe}\}_2$: 82 mg, $\{L^{Me2Te}\}_2$: 93 mg) was dissolved in 3 mL of a $CHCl_3$/MeOH mixture (1 : 2, v/v) and a 2 M solution of $LiBH_4$ in THF (0.2 mL, 0.4 mmol) was added dropwise in an atmosphere of dry argon. The reduction was completed when the yellow color of the diaryldiselenide or the red color of the ditelluride disappeared and a colorless solution was formed. Solid $[ReCl_3(PPh_3)_2(CH_3CN)]$ (85 mg; 0.1 mmol) was added to the solution. After 10 minutes, the formation of a dark precipitate was observed, which was filtered off, washed with 1 mL of MeOH, 2 mL of $Et_2O$ and dried under vacuum. Recrystallization from $CH_3CN/CHCl_3$ (1 : 1, v/v) by slow evaporation at −10 °C gave suitable single crystals for X-ray diffraction.

$[Re(PPh_3)(CH_3CN)(L^{HSe})_3]$ (**6**): Yield: 63 % (60 mg), purple solid. Elemental analysis: Calcd. for $C_{38}H_{33}NPReSe_3$: C, 47.7; H, 3.5; N, 1.5 %. Found: C, 47.7 %; H, 3.5 %; N, 1.3 %. IR (KBr, $cm^{-1}$): 3047 (w), 2270 (w), 1573 (m), 1471 (s), 1153 (s), 1019 (w), 997 (m), 738 (s), 509 (s). ESI+ MS (m/z): 940.9096 $[M\text{-}(MeCN)+Na]^+$ (calcd. 940.9008). $^1H$ NMR (600 MHz, $CDCl_3$) δ (ppm): 7.69–7.74 (m, 6H), 7.41–7.49 (m, 15H), 7.15–7.21 (m, 6H), 7.08–7.13 (m, 3H), 1.09 (s, 3H). $^{13}C\{^1H\}$ NMR (150 MHz, $CDCl_3$) δ (ppm): 147.1, 141.9, 134.8, 134.0, 129.3, 128.5, 128.1, 127.8, 127.7, 125.8, 1.9. $^{31}P\{^1H\}$ NMR (242 MHz, $CDCl_3$) δ (ppm): 16.3. $^{77}Se$ NMR (114 MHz, $CDCl_3$) δ (ppm): 975.1.

$[Re(PPh_3)(CH_3CN)(L^{Me2Se})_3]$ (**7**): Yield: 72 % (75 mg), purple solid. Elemental analysis: Calcd. for $C_{44}H_{45}NPReSe_3$: C, 50.7; H, 4.4; N, 1.3 %. Found: C, 50.7; H, 4.3; N, 1.2 %. IR (KBr, $cm^{-1}$): 3045 (w), 2968 (w), 2262 (w), 1573 (w), 1453 (m), 1185 (m), 1027 (w), 745 (s), 527 (s). ESI + MS (m/z): 1002.0141 $[M\text{–}(MeCN)+Na]^+$ (calcd. 1002.0169). $^1H$ NMR (600 MHz, $CDCl_3$) δ (ppm): 7.82–7.89 (m, 6H), 7.41–7.51 (m, 9H), 6.99 (t, $J=7.5$ Hz, 3H), 6.90 (d, $J=7.4$ Hz, 6H), 1.99 (s, 18H), 1.66 (s, 3H). $^{13}C\{^1H\}$ NMR (150 MHz, $CDCl_3$) δ (ppm): 146.5, 142.0, 141.5 134.9, 129.2, 127.7, 127.3, 126.3, 124.8, 23.6, 0.9. $^{31}P\{^1H\}$ NMR (242 MHz, $CDCl_3$) δ (ppm): 17.5. $^{77}Se$ NMR (114 MHz, $CDCl_3$) δ (ppm): 924.7.

$[Re(PPh_3)_2(L^{HTe})_3]$ (**8**): Yield: 51 % (67 mg), brown solid. Elemental analysis: Calcd. for $C_{54}H_{45}P_2ReTe_3$: C, 49.0; H, 3.4 %. Found: C, 48.5; H, 3.6 %. IR (KBr, $cm^{-1}$): 3047 (w), 1569 (w), 1479 (w), 1431 (s), 1316 (w), 1183 (w), 1088 (m), 729 (m), 692 (s), 509 (s). ESI+MS (m/z): 1348.0146 $[M+Na]^+$ (calcd. 1348.9592). $^1H$ NMR (400 MHz, $CDCl_3$) δ (ppm): 7.70–7.80 (m, 9H), 7.57–7.60 (m, 6H), 7.36–7.50 (m, 18H), 7.09–7.15 (m, 12H). $^{13}C\{^1H\}$ NMR (100 MHz, $CDCl_3$) δ (ppm): 138.3, 137.5, 134.7, 129.2, 128.5, 128.0, 127.7, 126.1. $^{31}P\{^1H\}$ NMR (160 MHz, $CDCl_3$) δ (ppm): 29.1 ($OPPh_3$), 19.8. $^{125}Te$ NMR (189 MHz, $CDCl_3$) δ (ppm): 1160.5, 419.4 $(PhTe)_2$.

$[Re(PPh_3)(CH_3CN)(L^{Me2Te})_3]$ (**9**): Yield: 56 % (66 mg), brown solid. Elemental analysis: Calcd. for $C_{44}H_{45}NPReTe_3$: C, 44.7; H, 3.8; N, 1.2 %. Found: C, 43.3; H, 3.8; N, 0.8 %. IR (KBr, $cm^{-1}$): 3043 (w), 2962 (w), 2256 (w), 1570 (w), 1478 (s), 1184 (w), 1027 (s), 744 (s), 527 (s). ESI+ MS (m/z): 1189.0025 $[M+H]^+$ (calcd. 1189.0076). $^1H$ NMR (600 MHz, $CDCl_3$) δ (ppm): 7.84–7.90 (m, 6H), 7.45–7.71 (m, 6H), 7.39–7.45 (m, 3H) 7.04 (t, $J=7.4$ Hz, 3H), 6.92 (d, $J=7.4$ Hz, 6H), 2.05 (s, 18H), 1.52 (s, 3H). $^{13}C\{^1H\}$ NMR (150 MHz, $CDCl_3$) δ (ppm): 144.2, 144.0, 143.7 135.4, 132.2, 129.2, 127.7, 127.0, 126.5, 27.6, 1.4. $^{31}P\{^1H\}$ NMR (242 MHz, $CDCl_3$) δ (ppm): 20.7. $^{125}Te$ NMR (189 MHz, $CDCl_3$) δ (ppm): 1302.6.

*[Re(PMe$_2$Ph)$_2$(L$^{Me2Se}$)$_3$] (**10**)*: $\{L^{Me2Se}\}_2$ (74 mg, 0.2 mmol) was dissolved in 3 mL of a $CHCl_3$/MeOH mixture (1 : 2, v/v) and a 2 M solution of $LiBH_4$ in THF (0.2 mL, 0.4 mmol) was added dropwise in an atmosphere of dry argon. The reduction was completed when the yellow color of the diselenide disappeared and a colorless solution was formed. Solid $[ReCl_3(PMe_2Ph_3)_3]$ (70 mg; 0.1 mmol) was added and the solution was heated on reflux for 30 min. The reaction mixture was filtered hot to remove LiCl. After cooling to room temperature, microcrystals were formed, which were washed with 2 mL of a mixture of MeOH/$Et_2O$ (1 : 1, v/v) and dried under vacuum. Recrystallization from a $CH_3CN/CH_2Cl_2$ mixture (1 : 1, v/v) at −10° C gave purple single crystals suitable for X-ray diffraction. Yield: 74 % (75 mg). Elemental analysis: Calcd. for $C_{40}H_{49}P_2ReSe_3$: C, 47.3; H, 4.9 %. Found: C, 47.4; H, 4.9 %. IR (KBr, $cm^{-1}$): 3043 (w), 2966 (w), 1574 (w), 1453 (m), 1091 (w), 1028 (m), 899 (s), 769 (m), 671 (w). ESI + MS (m/z): 877.9832 $[M\text{–}(PMe_2Ph)+H]^+$ (calcd. 877.9876). $^1H$ NMR (600 MHz, $CDCl_3$) δ (ppm): 7.86 (t, $J=7.7$ Hz, 2H), 7.20–7.30 (m, 4H), 7.06–7.19 (m, 9H), 7.01 (t, $J=7.1$ Hz, 2H), 6.88 (d, $J=6.3$ Hz, 2H), 2.24 (s, 6H), 2.17 (s, 6H), 1.85 (s, 12 H), 1.35 (d, $J=7.5$ Hz, 6H) . $^{13}C\{^1H\}$ NMR (150 MHz, $CDCl_3$) δ (ppm): 159.1, 154.6, 146.0, 145.3, 142.8, 142.0, 141.0, 131.4, 130.4, 129.1, 128.4, 128.2, 127.6, 127.4, 127.3, 127.1, 24.2, 23.3, 21.2, 20.8. $^{31}P\{^1H\}$ NMR (242 MHz, $CDCl_3$) δ (ppm): −31.8 (d, $^2J_{P-P}=232.1$ Hz), −33.7 (d, $^2J_{P-P}=231.9$ Hz). $^{77}Se$ NMR (114 MHz, $CDCl_3$) δ (ppm): 933.4, 920.1.

## Computational chemistry

The gas-phase geometry optimizations were performed at the B3LYP level using Gaussian based on initial guesses generated through GaussView at the high performance computing center of the Freie Universität Berlin supported by the Zentraleinrichtung für Datenverarbeitung Zedat (Curta).[61–66] Calculations were performed for the $[ReO(L)_4]^-$ ions with E = O, S, Se and Te, and for $[Re(ER)_3(PPh_3)(L)]$ complexes with E=O, S, Se, Te; R=Me, Ph, 2,6-$Me_2Ph$ and L = none (for R=Ph), $CH_3CN$ or $PPh_3$ and the free ligands $PPh_3$ and $CH_3CN$.

The double zeta basis LANL2DZ was applied for Re and the polarization augmented LANL2DZdp was applied for N, P, O, S, Se

and Te, where an effective core potential (ECP) was assumed for Re, P, S, Se and Te.[67–70] For C and H, the basis set 6-311G** was used.[71,72] All basis sets were obtained from the basis set exchange database.[73] Frequency calculations after the optimizations resulted in no negative frequencies for the converged geometries. The geometric parameters of the optimized and crystal structures match closely with maximum deviations of ca. 0.07 Å and 3°. Further evaluation of the results was performed using AIMUC, MultiWFN and Avogadro.[74–76] Details are given as Supporting material.

## Acknowledgements

*This work was supported by the Coordenadoria de Aperfeiçoamento de Pessoas de Nível Superior (CAPES/DAAD – Probral, n. 88887.314414/2019-00, Brazil), Conselho Nacional de Desenvolvimento Científico e Tecnológico (CNPq) and German Academic Exchange Service (DAAD, Germany). We gratefully acknowledge the assistance of the Core Facility BioSupraMol supported by the DFG and High-Performance-Computing (HPC) Centre of the Zentraleinrichtung für Datenverarbeitung (ZEDAT) of the Freie Universität Berlin for computational time and support. Open Access funding enabled and organized by Projekt DEAL.*

## Conflict of Interest

The authors declare no conflict of interest.

## Data Availability Statement

The data that support the findings of this study are available in the supplementary material of this article.

**Keywords:** arylselenolato ligands · aryltellurolato ligands · Density functional calculations · rhenium

[1] U. Abram, *Rhenium, in Comprehensive Coordination Chemistry II*, (ed. J. A. McCleverty, T. J. Meyer) Elsevier **2003**, Vol. 5, 271–402.
[2] A. Ibdah, S. Alduwikat, *J. Organomet. Chem.* **2017**, *842*, 9–20.
[3] C. A. Brown, M. Abrahamse, E. A. Ison, *Dalton Trans.* **2020**, *49*, 11403–11411.
[4] D. Wei, R. Buhaibeh, Y. Canac, J.-B. Sortais, *Molecules* **2021**, *26*, 2598.
[5] G. P. Connor, D. Delony, J. E. Weber, B. Q. Mercado, J. B. Curley, S. Schneider, J. M. Meyer, P. L. Holland, *Chem. Sci.* **2022**, *13*, 4010–4018.
[6] A. Pop, L. Wang, V. Dorcet, T. Roisnel, J.-F. Carpentier, A. Silvestry, Y. Sarazin, *Dalton Trans.* **2014**, *43*, 16459–16474.
[7] K. S. Moreira, A. Lunardi, G. F. Razera, N. V. Fagundes, C. N. Cechin, V. D. Schwade, R. Cargnelutti, E. S. Lang, B. Tirloni, *J. Mol. Struct.* **2021**, *1232*, 130083.
[8] F. D. da Silva, A. L. Hennemann, R. A. Burrow, E. S. Lang, U. Abram, S. S. dos Santos, *J. Cluster Sci.* **2022**, *33*, 815–824.
[9] C. N. Cechin, B. N. Cabral, F. Bublitz, T. Bortolotto, G. D. da Silveira, L. M. de Carvalho, R. Cargnelutti, U. Abram, S. Nakagaki, E. S. Lang, B. Tirloni, *New J. Chem.* **2021**, *45*, 19255.
[10] P. Bouziotis, I. Pirmettis, M. Pelecanou, C. P. Raptopoulou, A. Terzis, M. Papadopoulos, E. Chiotellis, *Chem. Eur. J.* **2001**, *7*, 3671–3680.
[11] Y. Chen, L. Zhang, Z. Chen, *Acta Crystallogr.* **2002**, *E58*, m590–m591.
[12] A. Meltzer, R. Cargnelutti, A. Hagenbach, E. S. Lang, U. Abram, *Z. Anorg. Allg. Chem.* **2015**, *641*, 2617–2623.
[13] J. D. Dilworth, J. Hu, J. R. Miller, D. L. Hughes, J. A. Zubieta, Q. Chen, *J. Chem. Soc. Dalton Trans.* **1995**, 3153–3164.
[14] J.-J. Peng, S.-M. Peng, G.-H. Hsiang, Y. Chi, *Organometallics* **1995**, *14*, 626–633.
[15] K. Chryssou, M. Pelecanou, I. C. Pirmettis, M. S. Papadopoulos, C. Raptopoulou, A. Terzis, E. Chiotellis, C. I. Stassinopoulou, *Inorg. Chem.* **2002**, *41*, 4478–4483.
[16] M. A. Alvarez, M. E. García, D. García-Vivó, E. Huergo, M. A. Ruiz, *Organometallics* **2018**, *37(20)*, 3425–3436.
[17] T.-F. Wang, C.-C. Wu, C.-W. Tsai, Y.-S. Wen, *Organometallics* **1998**, *17*, 131–138.
[18] W.-F. Liaw, Y.-C. Horng, D.-S. Ou, C.-Y. Chuang, C.-K. Lee, G.-H. Lee, S.-M. Peng, *J. Chin. Chem. Soc.* **1995**, *42*, 59–65.
[19] A. A. Pasynskii, Y. V. Torubaev, A. V. Pavlova, I. V. Skabitsky, G. L. Denisov, V. A. Grinberg, *J. Cluster Sci.* **2015**, *26*, 247–255.
[20] M. Karthikeyan, R. Govindarajan, E. Duraisamy, V. Veena, N. Sakthivel, B. Manimaran, *Chem. Select* **2017**, *2*, 3362–3368.
[21] A. Vanitha, S. M. Mobin, B. Manimaran, *Organomet. Chem.* **2011**, *696*, 1609–1617.
[22] F. A. Cotton, K. R. Dunbar, *Inorg. Chem.* **1987**, *26*, 1305–1309.
[23] H. Egold, S. Klose, U. Flörke, *Z. Anorg. Allg. Chem.* **2001**, *627*, 164-xx.
[24] R. Nagarajaprakash, C. A. Kumar, S. M. Mobin, B. Manimaran, *Organometallics* **2015**, *34*, 724.
[25] B. Manimaran, A. Vanitha, M. Karthikeyan, B. Ramakrishna, S. M. Mobin, *Organometallics* **2014**, *35*, 465–472.
[26] H. Egold, U. Flörke, *Z. Anorg. Allg. Chem.* **2001**, *627*, 2295–3205.
[27] L. Veronese, E. Q. Procopio, D. Manggioni, P. Mercandelli, M. Pinigati, *New J. Chem.* **2017**, *41*, 11268.
[28] A. A. Pasynskii, Y. V. Torubaev, A. V. Pavlova, S. S. Shapovalov, I. V. Skabitskii, G. L. Denisov, *Russ. J. Coord. Chem.* **2014**, *40*, 611–616.
[29] A. A. Pasynskii, S. S. Shapovalov, I. V. Skabitskii, O. G. Tikhonova, T. K. Krishtop, *Russ. J. Coord. Chem.* **2015**, *41*, 76–79.
[30] A. Vanitha, J. Muthukumaran, R. Krishna, B. Manimaran, *Acta Crystallogr.* **2010**, *E66*, m518.
[31] J. Muthukumaran, M. Kannan, A. Vanitha, B. Manimaran, R. Krishna, *Acta Crystallogr.* **2010**, *E66*, m558.
[32] L. Veronese, E. Q. Procopio, D. Magioni, P. Mercandelli, M. Panigati, *New J. Chem.* **2017**, *41*, 11268–11279.
[33] M. Karthikeyan, R. Govindarajan, C. A. Kumar, U. Kumar, B. Manimaran, *J. Organomet. Chem.* **2018**, *866*, 27–34.
[34] T. Fietz, H. Spies, P. Leibnitz, D. Scheller, *J. Coord. Chem.* **1996**, *38*, 227–235.
[35] F. De Montigny, L. Guy, G. Pilet, N. Vanthuyne, G. Roussel, R. Lombardi, T. B. Freedman, L. A. Nafie, J. Crassous, *Chem. Commun.* **2009**, 4841–4843.
[36] H. Herberhold, G. X. Jin, W. Milius, *Z. Anorg. Allg. Chem.* **1994**, *620*, 1295–1300.
[37] R. Cervo, T. R. R. Lopes, A. R. de Vasconcelos, J. F. Cargnelutti, R. F. Schumacher, B. Tirloni, S. S. dos Santos, U. Abram, E. S. Lang, R. Cargnelutti, *New J. Chem.* **2021**, *45*, 12863–12870.
[38] M. Roca Jungfer, A. Hagenbach, E. Schulz Lang, U. Abram, *Eur. J. Inorg. Chem.* **2019**, 4974–4984.
[39] V. D. Schwade, A. Hagenbach, E. S. Lang, K. Klauke, F. Mohr, U. Abram, *Eur. J. Inorg. Chem.* **2014**, 1949–1954.
[40] R. Cargnelutti, E. S. Lang, P. Piquini, U. Abram, *Inorg. Chem. Commun.* **2014**, *45*, 48–50.
[41] B. N. Cabral, L. Kirsten, A. Hagenbach, P. Piquini, M. Patzschke, E. S. Lang, U. Abram, *Dalton Trans.* **2017**, *46*, 9280–9286.
[42] W. S. Haller, K. J. Irgolic, *J. Organomet. Chem.* **1972**, *38*, 97–103.
[43] A. C. McDonell, T. W. Hambley, M. R. Snow, A. G. Wedd, *Aust. J. Chem.* **1983**, *36*, 253–258.
[44] P. J. Blower, J. R. Dilworth, J. Hutchinson, T. Nicholson, J. Zubieta, *Inorg. Chim. Acta* **1984**, *90*, L27–L30.
[45] T. Nicholson, P. Lombardi, J. Zubieta, *Polyhedron* **1987**, *6*, 1577–1585.
[46] E. Block, H. Kang, G. Ofori-Okai, J. Zubieta, *Inorg. Chim. Acta* **1989**, *156*, 27–28.
[47] M. Li, A. Ellern, J. H. Espenson, *Inorg. Chem.* **2005**, *44*, 3690–3699.
[48] J. R. Dilworth, C. Lu, Y. Zheng, J. Zubieta, *Polyhedron* **1999**, *18*, 501–510.
[49] M. Papadopoulos, C. Tsoukalas, B. Nock, T. Maina, C. P. Raptopoulou, H.-J. Pietzsch, M. Friebe, H. Spies, B. Johannsen, E. Chiotellis, *Inorg. Chim. Acta* **1999**, *295*, 1–8.
[50] J. Arnold, *Prog. Inorg. Chem.* **1995**, *43*, 353–418.
[51] G. Wilkinson, G. Rouschias, *J. Chem. Soc. A* **1967**, 993–1000.
[52] P. J. Blower, J. R. Dilworth, *J. Chem. Soc. Dalton Trans.* **1985**, 2305–2309.

[53] P. J. Blower, J. R. Dilworth, J. Hutchinson, T. Nicholson, J. A. Zubieta, *J. Chem. Soc. Dalton Trans.* **1985**, 2639–2645.
[54] N. de Vries, J. C. Dewan, A. G. Jones, A. Davison, *Inorg. Chem.* **1988**, *27*, 1574–1580.
[55] G. W. Parshall, L. W. Shive, F. A. Cotton, *Inorg. Synth.* **1977**, *17*, 110–112.
[56] G. Wilkinson, G. Rouschias, *J. Chem. Soc. A* **1967**, 993–1000.
[57] J. Chatt, G. J. Leigh, D. M. P. Mingos, R. J. Paske, *J. Chem. Soc. A* **1968**, 2636–2641.
[58] G. M. Sheldrick, *Acta Crystallogr.* **2008**, *A64*, 112–122.
[59] O. V. Dolomanov, L. J. Bourhis, R. J. Gildea, J. A. K. Howard, H. Puschmann, *J. Appl. Crystallogr.* **2009**, *42*, 339–341.
[60] *Diamond – Crystal and Molecular Structure Visualization*, Crystal Impact, Dr. H. Putz & Dr. K. Brandenburg GbR, Bonn, Germany, vers. 4.6.5, 2021.
[61] R. Dennington, T. A. Keith, J. M. Millam, *GaussView, Version 6*, Semichem Inc., Shawnee Mission, KS **2016**.
[62] High performance computing (HPC) system Curta at Freie Universität Berlin. DOI: 10.17169/refubium-26754.
[63] M. J. Frisch, G. W. Trucks, H. B. Schlegel, G. E. Scuseria, M. A. Robb, J. R. Cheeseman, G. Scalmani, V. Barone, G. A. Petersson, H. Nakatsuji, X. Li, M. Caricato, A. V. Marenich, J. Bloino, B. G. Janesko, R. Gomperts, B. Mennucci, H. P. Hratchian, J. V. Ortiz, A. F. Izmaylov, J. L. Sonnenberg, D. Williams-Young, F. Ding, F. Lipparini, F. Egidi, J. Goings, B. Peng, A. Petrone, T. Henderson, D. Ranasinghe, V. G. Zakrzewski, J. Gao, N. Rega, G. Zheng, W. Liang, M. Hada, M. Ehara, K. Toyota, R. Fukuda, J. Hasegawa, M. Ishida, T. Nakajima, Y. Honda, O. Kitao, H. Nakai, T. Vreven, K. Throssell, J. A. Montgomery Jr., J. E. Peralta, F. Ogliaro, M. J. Bearpark, J. J. Heyd, E. N. Brothers, K. N. Kudin, V. N. Staroverov, T. A. Keith, R. Kobayashi, J. Normand, K. Raghavachari, A. P. Rendell, J. C. Burant, S. S. Iyengar, J. Tomasi, M. Cossi, J. M. Millam,M. Klene, C. Adamo, R. Cammi, J. W. Ochterski, R. L. Martin, K. Morokuma, O. Farkas, J. B. Foresman, J. Fox, *Gaussian 16, Revision B.01*, Gaussian, Inc., Wallingford CT **2016**.
[64] S. H. Vosko, L. Wilk, M. Nusair, *Can. J. Phys.* **1980**, *58*, 1200–1211.
[65] A. D. Becke, *J. Chem. Phys.* **1993**, *98*, 5648–5652.
[66] C. Lee, W. Yang, R. G. Parr, *Phys. Rev.* **1988**, *B37*, 785–789.
[67] W. R. Wadt, P. J. Hay, *Chem. Phys.* **1985**, *82*, 284–298.
[68] P. J. Hay, W. R. Wadt, *Chem. Phys.* **1985**, *82*, 299–310.
[69] C. E. Check, T. O. Faust, J. M. Bailey, B. J. Wright, T. M. Gilbert, L. S. Sunderlin, *J. Phys. Chem. A* **2001**, *105*, 8111–8116.
[70] T. H. Dunning, P. J. Hay, *Mod. Theor. Chem.* **1977**, *3*, 1–27.
[71] R. Krishnan, J. S. Binkley, R. Seeger, J. A. Pople, *J. Chem. Phys.* **1980**, *72*, 650–654.
[72] T. Clark, J. Chandrasekhar, G. W. Spitznagel, P. V. R. Schleyer, *J. Comput. Chem.* **1983**, *4*, 294–301.
[73] K. L. Schuchardt, B. T. Didier, T. Elsethagen, L. Sun, V. Gurumoorthi, J. Chase, J. Li, T. L. Windus, *J. Chem. Inf. Model.* **2007**, *47*, 1045–1052.
[74] T. Lu, F. Chen, *J. Comput. Chem.* **2012**, *33*, 580–592.
[75] D. Vega, D. Almeida, *J. Comput. Methods Sci. Eng.* **2014**, *14*, 131–136.
[76] C. S. López, A. R. de Lera, *Curr. Org. Chem.* **2011**, *15*, 3576–3593.
[77] S. Jenkins, P. W. Ayers, S. R. Kirk, P. Mori-Sánchez, A. M. Pendás, *Chem. Phys. Lett.* **2009**, *471*, 174–177.
[78] E. Espinosa, I. Alkorta, J. Elguero, E. Molins, *J. Chem. Phys.* **2002**, *117*, 5529–5542.
[79] M. D. Hanwell, D. E. Curtis, D. C. Lonie, C. Vandermeersch, E. Zurek, G. R. J. Hutchison, *J. Cheminf.* **2012**, *4*, 17.

Manuscript received: January 11, 2023
Revised manuscript received: January 28, 2023
Accepted manuscript online: January 30, 2023